Identifying growth mechanisms for laser-induced magnetization in FeRh

Please check the document version of this publication:

• A submitted manuscript is the version of the article upon submission and before peer-review. There can be important differences between the submitted version and the official published version of record. People interested in the research are advised to contact the author for the final version of the publication, or visit the DOI to the publisher's website.
• The final author version and the galley proof are versions of the publication after peer review.
• The final published version features the final layout of the paper including the volume, issue and page numbers.

Link to publication

Identifying growth mechanisms for laser-induced magnetization in FeRh

Bastiaan Bergman,[1,2,*] Ganping Ju,[2] Julius Hohlfeld,[2] René J. M. van de Veerdonk,[2] Jai-Young Kim,[2] Xiaowei Wu,[2]
Dieter Weller,[2] and Bert Koopmans[1]

[1]*Department of Applied Physics and Center for NanoMaterials (cNM), Eindhoven University of Technology,*
P.O. Box 513, 5600 MB Eindhoven, The Netherlands
[2]*Seagate Research, 1251 Waterfront Place, Pittsburgh, Pennnsylvania 15222, USA*
(Received 17 October 2005; published 17 February 2006)

Time-resolved pump-probe measurements of the magnetic phase change from paramagnetic to ferromagnetic and back in FeRh thin films are presented. Data are compared with simulations of laser-induced magnetization dynamics using the Landau-Lifshitz-Gilbert equation with a time dependent magnetization density, responding to the evolution of the thermal profile throughout the film. We demonstrate that the observed magneto-optical transients should be interpreted in terms of an interplay between the local magnetic moment, nonlocal domain growth or alignment, and magnetization precession as launched by the varying demagnetizing fields. Kerr rotation and reflectivity are shown to provide a complementary view on the phase transition.

PACS number(s): 75.30.Kz, 75.40.Gb, 75.50.Ss, 78.47.+p

An appealing area of research has been opened by recent studies that showed the feasibility of manipulating magnetic matter at down to sub-ps time scales by laser heating with femtosecond laser pulses. In pioneering work, Beaurepaire *et al.* demonstrated that the magnetic moment of ferromagnetic thin films could be quenched well within a ps after laser excitation,[1] as confirmed later by several groups.[2–5] The reverse process, the ultrafast *generation* of ferromagnetic order has been a quest since then. Cooling down from above the Curie temperature, as applied in thermomagnetic writing, is hindered by the cooling rate, and usually limited to 10–100 s of picoseconds.[6]

Very recently, two groups independently showed the possibility of generating ferromagnetic order at a sub-ps time scale in FeRh thin films.[7,8] FeRh is a particularly interesting system that displays an antiferromagntic (AF) phase below, and a ferromagnetic (F) phase above a phase transition temperature (T_P) around 370 K, depicted in Fig. 1(b). Laser heating such a film, and thus driving it through its AF to F phase transition,[8] showed a first onset of ferromagnetism within the first ps, which implied the phase transition to be of electronic origin. On a longer time scale a continued growth of F order is witnessed, possibly due to a domain expansion or alignment. Not only does FeRh provide a unique model system for improving our theoretical understanding of (sub-)ps magnetic processes, it also receives considerable interest for its potential application in heat-assisted magnetic recording.[9,10]

In this Rapid Communication we provide additional experimental time-resolved magneto-optical Kerr effect (TRMOKE) data, as well as numerical modeling thereof. The latter accounts for an interplay between laser heating, thermal diffusion, as well as the magnitude and orientation of induced magnetic moments in FeRh thin films after laser irradiation. In particular, we unambiguously demonstrate the occurrence of a magnetization precession launched by the rapid growth of the demagnetizing field during the buildup of magnetic order in the film. Figure 1 schematically illustrates these effects, discussed in more detail further on.

We claim that including such effects is of crucial importance for deriving quantitative information from the TRMOKE data, as obviously required to further enhance our understanding of the ultrafast magnetic process in the system.

$Fe_{45}Rh_{55}$ thin film samples (thickness 100 nm) were made with dc-magnetron sputtering on a MgO substrate, following procedures reported before.[8] Vibrating sample magnetometery (VSM) displayed a phase transition at 350 K, and a hysteresis of $\sim$10 K as usually observed for such films. TRMOKE was performed with 800 nm pump laser pulses ($\sim$80 fs, 8 MHz rep. rate) and time delayed second harmonic probe laser pulses of 400 nm. Typically, we used pump powers between 0 and 15 mW, and laser spot diameters of 6 and 3 micrometers, for pump and probe, respectively. Experiments are performed in a magnetic field H_a applied at an angle of 45° with respect to the surface normal.
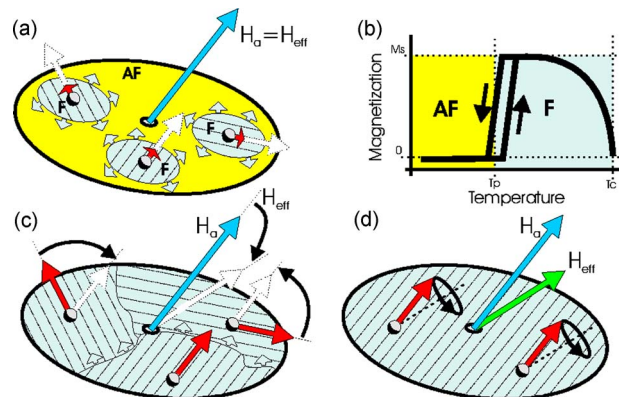
FIG. 1. (Color online) Growth of local magnetization and areal growth of the *F* phase (a), is followed by a growth of net magnetization by alignment of individual domains, the demagnetization field grows equally, leading to a canting total effective field (c), the homogeneous magnetization starts precessing around the new effective field (d). Red (dark gray) vectors represent the local magnetization $\vec{\mathcal{M}}(\vec{r},t)$. FeRh is antiferromagnetic below and ferromagnetic above the transition temperature T_p, the phase transition shows some temperature hysteresis (b).

FIG. 2. (Color online) Transient Kerr rotation measured at 3.5 kG as a function of time. Applied pump power varies from 1.3 mW for the lowest curve to 16.5 mW for the highest curve (a). Peak height of the first and the second peaks plotted against the pump power applied (b). Corresponding simulations, as discussed in the text, are represented in (c) and (d).

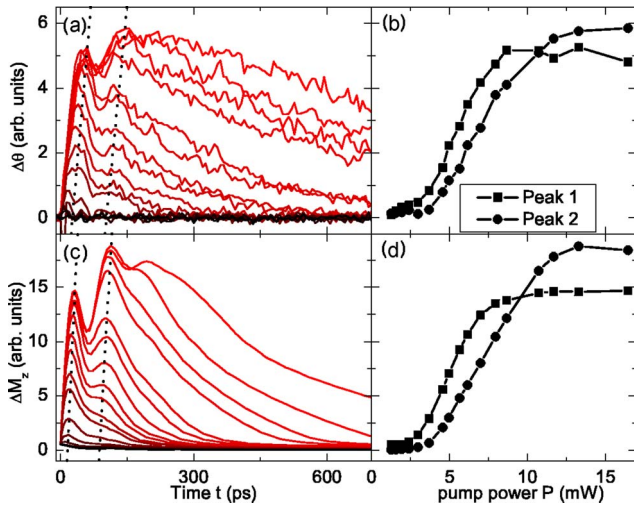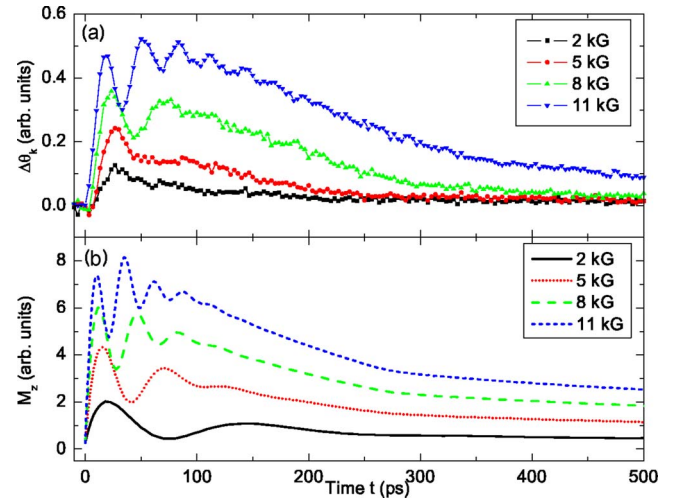FIG. 3. (Color online) Transient Kerr rotation measured with an external applied field of 2 to 11 kG at 8 mW pump power (a) and simulation thereof using the assumptions as described (b).

The probe angle of incidence is 45°, colinear with the applied field. It was verified that in this configuration, the Kerr rotation, detected with a Wollaston differential detection, is dominated by the perpendicular component of the magnetization. In order to derive information on the electron and lattice dynamics, the transient reflectivity was recorded simultaneously with the TRMOKE. For more details we refer to Ref. 8.

In Fig. 2(a) the Kerr rotation during the first 700 ps after pump excitation of a 100 nm FeRh film is presented for increasing pump powers. We note that the fast nucleation of ~20% of the final magnetic order during the first ps, reported before,[8] is not separately recognizable in this long time scan. A clear threshold behavior is elucidated in the representation of Fig. 2(b), where the height of two features (indicated by the dashed lines in *A*) is plotted against the pump power. A minimum power of ~3 mW is found to be required to pass the transition temperature, and only for higher powers a finite laser-induced Kerr rotation is being witnessed. We stress that the observation of a threshold power is considered as an essential fingerprint of the laser-induced phase transition. As a second signature of driving the film into the ferromagnetic phase, the duration over which the induced Kerr signal lasts increases as a function of pump fluence (up to nanoseconds at our highest fluences), because it takes increasingly longer before the magnetic film is cooled down below the phase transitions by diffusive cooling.

As to the observation of two successive peaks in the data at the highest fluency, it has been argued before[7,8] that such a behavior could be expected because within a complete heating cycle the film passes the transition temperature twice, and at temperatures above T_P the magnetization is a monotonously decreasing function. Data of Fig. 3(a), in which the transient Kerr rotation is presented for different applied fields at constant pump power, seem to contradict this interpreta-

tion. Clearly, at high fields the precession gets more pronounced and also the precession frequency increases with the applied field. This would rather indicate an effect of (heavily damped) precessive origin, in which a field dependent Larmor frequency is observed. The forthcoming analysis will show that this is indeed the correct interpretation.

We conjecture that a proper interpretation of the Kerr transients requires three magnetic phenomena: (i) dynamics of the magnitude of the local magnetization, (ii) the growth or alignment of regions with differently oriented magnetization towards a homogeneous single domain state, and (iii) the precession of the average magnetization in the effective field, depicted by Figs. 1(a), 1(c), and 1(d) respectively. We present a formal description of these processes for a thin film with surface normal $\hat{z}$, and a local magnetization $\vec{\mathcal{M}}(\vec{r},t)$ driven by the laser-induced temperature transient $T(z,t)$. Note that the lateral size of the heated volume is much larger than the thickness of it and therefore pure one-dimensional heat diffusion will be assumed.

First, we analyze the *magnitude* $\mathcal{M}(\vec{r},t)$ of $\vec{\mathcal{M}}(\vec{r},t)$. By laser excitation, hot electrons are excited that in ferromagnetic transition metals thermalize within ~100 fs.[1] After thermalization, an electron (T_e), lattice (T_l), and spin (T_s) temperature can be defined within a three-temperature model.[1] From previous experiments it was concluded that it is the thermalized electron gas, rather than the successively heated lattice, that drives the phase transition in FeRh.[7,8]

According to the three-temperature model, we can describe the convergence of the local T_s with T_e at a spin relaxation time τ_s by: $\dot{T}_s(\vec{r},t)=[T_e(\vec{r},t)-T_s(\vec{r},t)]/\tau_s$. Then in a first scenario, it would be tempting to describe the evolution of the local magnetic moments by $\mathcal{M}(\vec{r},t)=M_{eq}[T_s(\vec{r},t)]$. Here, M_{eq} represents the equilibrium magnetization at temperature T_s, with $M_{eq}=0$ for $T_s<T_P$. However, it may be considered more realistic from a physics point of view that the local magnetic order grows monotonously to an optimum at the spin temperature, a behavior that should be described by $\dot{\mathcal{M}}(\vec{r},t)=[M_{eq}(T_s(z,t))-\mathcal{M}(\vec{r},t)]/\tau_m$, defining an additional time scale τ_m.

Combining the two scenarios, a large τ_s, larger than τ_m, would make the magnetization to go twice through a maximum—i.e., during heat-up as well as while cooling down— as argued before.[7,8] However, if this would be the cause of the second peak in the transient Kerr data then one would expect it to shift in time relative to the first peak with increasing pump power. Since such a shift is not observed in Fig. 2(a) at all, τ_s must be smaller than τ_m. A larger τ_m in its turn ($\tau_m \gg \tau_s$), accounts for the gradual growth of the magnetization without the implication of a relative time shift for the second peak with increasing fluence. In the forthcoming analysis we neglect τ_s (i.e., set $\tau_s=0$).

Secondly, it may be expected that the initial phase transition occurs in a nonhomogeneous way, leading to separate domains with different *orientations* of the magnetic moment. Although the applied magnetic field will lead to a finite spatially averaged moment, the Zeeman splitting will be insufficient to fully align all domains at this early stage. However, as soon as neighboring domains get in direct contact, exchange forces will cause a rapid alignment of the domains. Thus, a laterally averaged magnetization $\vec{M}(z,t) = A^{-1} \int \vec{\mathcal{M}}(\vec{r},t) dx\, dy$ will develop that is collinear over the whole sample, though its magnitude is a function of z due to the nonhomogeneous thermal profile. Defining a time scale τ_M, its dynamics is given by: $\dot{M}(z,t) = [A^{-1} \int \mathcal{M}(\vec{r},t) dx\, dy - M(z,t)]/\tau_M$.

Thirdly, the pronounced time dependence of the magnetic moment has a strong effect on the demagnetization fields (i.e. the shape anisotropy). Initially, when only a little net magnetic moment has built up, the effective field is entirely dominated by the Zeeman energy associated with the applied magnetic field canted out of the film plane. After the first alignment, a demagnetization field will build up that tends to pull the magnetization inplane. As demonstrated in many recent studies in which local anisotropies are affected by rapid laser heating, such a situation leads to a precessing magnetization.[11–14] The precessional dynamics is described by an effective field $\vec{H}_{eff}(t) = \vec{H}_a - \hat{z} \int M_z^2(z,t) dz / \int M_z(z,t) dz$, and the Landau-Lifzhitz-Gilbert equation in terms of the normalized magnetization $\vec{m}(t) = \vec{M}(z,t)/M(z,t)$:

$$\frac{d\vec{m}}{dt} = \gamma \mu_0 (\vec{m} \times \vec{H}_{eff}) + \alpha \left(\vec{m} \times \frac{d\vec{m}}{dt} \right), \quad (1)$$

with α the dimensionless Gilbert damping, γ_0 the gyromagnetic ratio, and μ_0 the magnetic permeability of vacuum.

Finally, the driving force for the whole magnetization dynamics, i.e., the evolution of the temperature profile $T(z,t)$, has to be evaluated. We assume that at $t=0$ heat is instantaneously deposited in the film with an extinction depth δ_0 and has a Gaussian distribution over depth. Heat diffusion is a sufficiently slow process to neglect the subsystems, therefore $T_e = T_l = T_s$ is assumed. The temperature evolution is given by the one-dimensional heat diffusion of a Gaussian distribution:

$$\Delta T(z,t) = \frac{\delta_0 \cdot T_{max}}{\sqrt{4Dt + \delta_0^2}} e^{-z^2/(4Dt + \delta_0^2)}, \quad (2)$$

where $\Delta T = T_{max} - T_0$ with T_0 the environment temperature and T_{max} the maximum temperature reached upon laser illu-

mination and D is the diffusion coefficient in (m^2/s). The extinction depth is calculated from the skin depth in metals, in our case and for 800 nm: $\delta_0 \approx 30$ nm. We obtained $D=2 \times 10^{-5}$ m^2/s by fitting the transient reflectivity data obtained at a fluence below threshold, where the phase change certainly does not play a role. Furthermore, the maximum temperature reached (at the max. fluence of 16.5 mW) and the ambient temperature (above room temperature because of the high repetition rate) are found to be ∼420 K and ∼330 K, respectively, by fitting the full model to the data of Figs. 2(a) and 2(b) and using $T_P = 350$ K.

It is of importance to note that by applying our model to the transient Kerr measurement, we cannot distinguish between the different causes of net growth of magnetization, $M(t)$. Therefore we introduced an overall time constant τ_K: $\dot{\vec{M}}(z,t) = [M_{eq}(T_e(z,t)) \cdot \vec{m}(t) - \vec{M}(z,t)]/\tau_K$, that accounts for effects related to both τ_m and τ_M. We first solve this differential equation, using $M_{eq}(T)$ from the VSM data upon neglecting hysteresis. Then, the calculated evolution of $M(z,t)$ is used as input for the LLG equation and as a boundary condition, assuming $\vec{m}$ along $\vec{H}_a$ upon nucleation.

Finally, the Kerr transient is calculated using a finite penetration depth of the probe laser pulse, i.e., using a weighted average over the full skin depth. Figures 2(c), 2(d), and 3(b) show a full simulation of the phase change upon laser heating for the same set of increasing pump powers [2(c) and 2(d)] and applied fields Fig. 3(b) as used for the measurements. Comparison reveals that many qualitative features in the measurement are reproduced by the simulation, including the threshold behavior, the relative amplitude of the first and second peak, as well as the appearance of a weak third feature at the highest fluence. The Gilbert damping α and time constant τ_K were adjusted for maximum agreement with the experiment. This gives $\alpha=0.3$ and $\tau_K=50$ ps. The damping is higher than most commonly reported values on the Gilbert damping in ferromagnetic materials. Besides pure material specific the high value can also be explained with the possibly high degree of incoherence in the precession caused by the nonuniform heating and partial transition, back to the AF phase.

After having demonstrated the semiquantitative agreement of our precession-based model with the TRMOKE data, we analyze the transient *reflectivity* recorded simultaneously. The transient reflectivity has two contributions here. First, a contribution due to the increased electron temperature and the continuous lattice expansion. Secondly, the AF to F phase change is accompanied by an abrupt change in the lattice constant and, possibly, in the electronic structure, resulting in a changed reflectivity for fluences above threshold. In Fig. 4(a) the reflectivity at low pump power, well below the transition temperature, is normalized to its peak value and subtracted from normalized reflectivity graphs at higher pump powers. Left over in these graphs is just the phase change contribution to the transient reflectivity (shaded area in inset). The dynamics displayed by this component is expected to closely follow the scalar average of the magnitude of the local magnetization $\mathcal{M}(z,t)$, delayed by some finite response time of the lattice, τ_L, but not affected by the gradual alignment process (as described by τ_M). Thereby, it
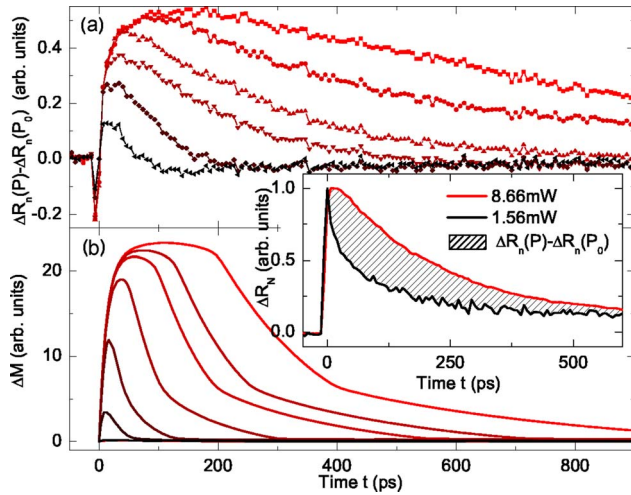
FIG. 4. (Color online) Difference of normalized transient reflectivity at a fluence power of 3.7 to 16.5 mW and the normalized reflectivity at the lowest power where the temperature stays below the transition temperature, measured with an applied field of 3.5 kG (a) Simulation of magnitude of the local magnetic moment at $z=0$ (b).

can be simulated by a simple differential equation: $\dot{\mathcal{M}}(z,t) = [M_{eq}(T_e(z,t)) - \mathcal{M}(z,t)]/\tau_R$, where we can assume $\tau_R^{-1} \approx \tau_m^{-1} + \tau_L^{-1}$.

Results are displayed in Fig. 4(b). The magnitude of magnetization grows initially with the same speed for all applied pump powers, only the magnitude of the magnetization changes. At higher power, FeRh stays longer above the transition temperature, T_P, and therefore has more time to grow its ferromagnetic phase. At highest power the sample is heated well above the transition temperature and a lower

magnetization is initially reached due to a partial quenching of the magnetization. Thereafter, while the sample cools down to the transition temperature, the magnetization grows further until a maximum is reached. Note that the magnetization does not go through a maximum before it is quenched, supporting the assumption that τ_s can be neglected.

Interestingly, we found that a satisfactory fit could only be obtained for $\tau_R \approx 1/(\tau_m^{-1} + \tau_L^{-1}) = 10$ ps that is significantly shorter than the $\tau_K = 50$ ps from the TRMOKE data. This unambiguously shows that $\tau_m \ll \tau_M$, an observation that is consistent with a scenario in which the slow response of the transient Kerr signal is almost entirely due to the aligning process, i.e., $\tau_K \approx \tau_M$.

In conclusion, we compared TRMOKE and transient reflectivity experiments with simulations that include magnetization growth and alignment processes as well as a full orientational evaluation through LLG dynamics. We provided strong evidence that an initial rapid growth of magnetic moment within at most 10 ps is followed by a gradual alignment process where local magnetic moments are aligned relative to each other in about 50 ps. Furthermore, it was found that transient Kerr and reflectivity provide a different view on the laser-induced magnetization dynamics. The first one is sensitive to the perpendicular component of the vectorial average of magnetization while the latter is sensitive to the magnitude of magnetization only. Such data are considered of crucial relevance for further increasing our understanding of the exciting laser-induced phase transition in FeRh.

*Electronic address: B.Bergman@us.ibm.com

[1] E. Beaurepaire, J.-C. Merle, A. Daunois, and J.-Y. Bigot, Phys. Rev. Lett. **76**, 4250 (1996).

[2] J. Hohlfeld, E. Matthias, R. Knorren, and K. H. Bennemann, Phys. Rev. Lett. **78**, 4861 (1997).

[3] E. Beaurepaire, M. Maret, V. Halte, J.-C. Merle, A. Daunois, and J.-Y. Bigot, Phys. Rev. B **58**, 12134 (1998).

[4] J. Gudde, U. Conrad, V. Jahnke, J. Hohlfeld, and E. Matthias, Phys. Rev. B **59**, R6608 (1999).

[5] B. Koopmans, M. van Kampen, J. T. Kohlhepp, and W. J. M. de Jonge, Phys. Rev. Lett. **85**, 844 (2000).

[6] J. Hohlfeld, T. Gerrits, M. Bilderbeek, T. Rasing, H. Awano, and N. Ohta, Phys. Rev. B **65**, 012413 (2001).

[7] J.-U. Thiele, M. Buess, and C. H. Back, Appl. Phys. Lett. **85**, 2857 (2004).

[8] G. Ju, J. Hohlfeld, B. Bergman, R. J. M. van de Veerdonk, O. N. Mryasov, J.-Y. Kim, X. Wu, D. Weller, and B. Koopmans, Phys. Rev. Lett. **93**, 197403 (2004).

[9] J.-U. Thiele, S. Maat, and E. E. Fullerton, Appl. Phys. Lett. **82**, 2859 (2003).

[10] J.-U. Thiele, S. Maat, J. L. Robertson, and E. E. Fullerton, IEEE Trans. Magn. **40**, 2537 (2004).

[11] M. van Kampen, C. Jozsa, J. T. Kohlhepp, P. LeClair, L. Lagae, W. J. M. de Jonge, and B. Koopmans, Phys. Rev. Lett. **88**, 227201 (2002).

[12] M. van Kampen, Ph.D. Thesis, TUe, Eindhoven (2003).

[13] G. Ju, A. V. Nurmikko, R. F. C. Farrow, R. F. Marks, M. J. Carey, and B. A. Gurney, Phys. Rev. Lett. **82**, 3705 (1999).

[14] Q. Zhang, A. V. Nurmikko, A. Anguelouch, G. Xiao, and A. Gupta, Phys. Rev. Lett. **89**, 177402 (2002).